Supplementary Information for

A 30 m annual cropland dataset of China from 1986 to 2021

Table of contents

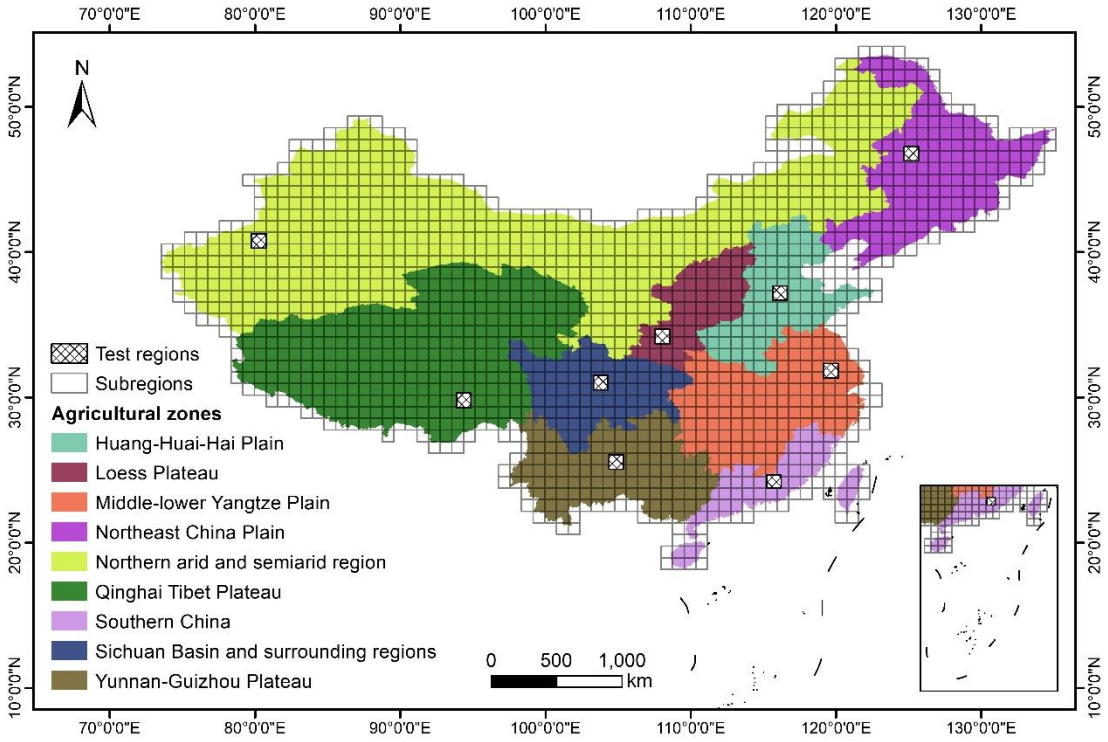

Figure S1. Divisions of the study area. Annual cropland classification is performed within each 0.8°×0.8° subregion. Test regions with a size of 100 km×100 km are used to find the best LandTrendr arguments for each agricultural zone.

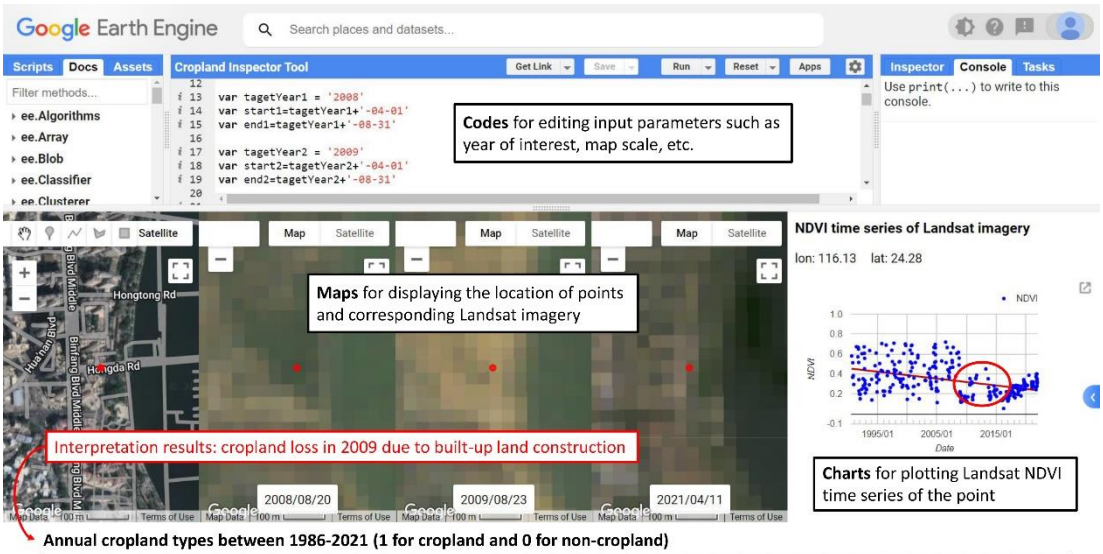

Point Id	86	87	88	89	90	91	92	93	94	95	96	97	98	99	00	01	02	03	04	05	06	07	08	09	10	11	12	13	14	15	16	17	18	19	20	21
29	1	1	1	1	1	1	1	1	1	1	1	1	1	1	1	1	1	1	1	1	1	1	1	0	0	0	0	0	0	0	0	0	0	0	0	0

Figure S2. An example of the sample interpretation process using the developed Cropland Inspector Tool on © Google Earth Engine (https://code.earthengine.google.com/616d493de325aaa5e3316a58ed8e7531). The location was covered by croplands before 2009 but converted to built-up areas since then, of which changes were clearly shown in Landsat images and NDVI time series.

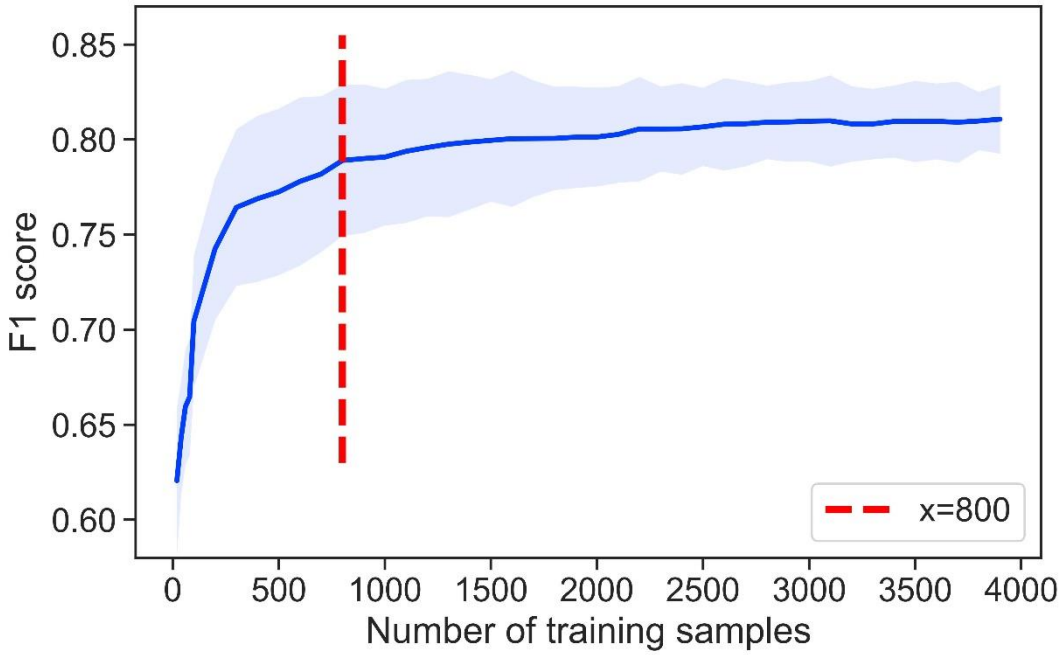

Figure S3. Mean F1 score of annual cropland classification results under different training sample sizes.

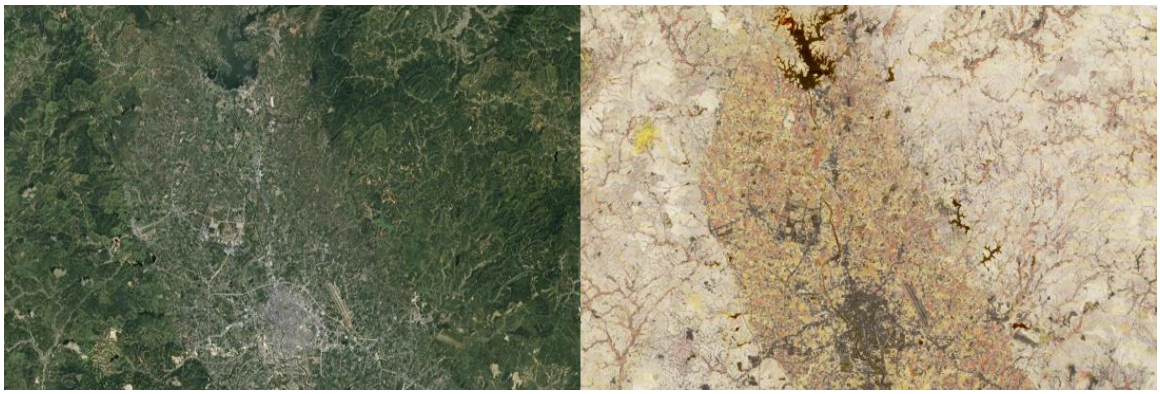

Figure S4. A comparison of a true color Landsat imagery displayed (left) and a corresponding NDVI composite imagery (with 10th, 50th, and 90th percent quantile of one-year values as the RGB channels) on the right. The Landsat imagery is provided by USGS with free access.

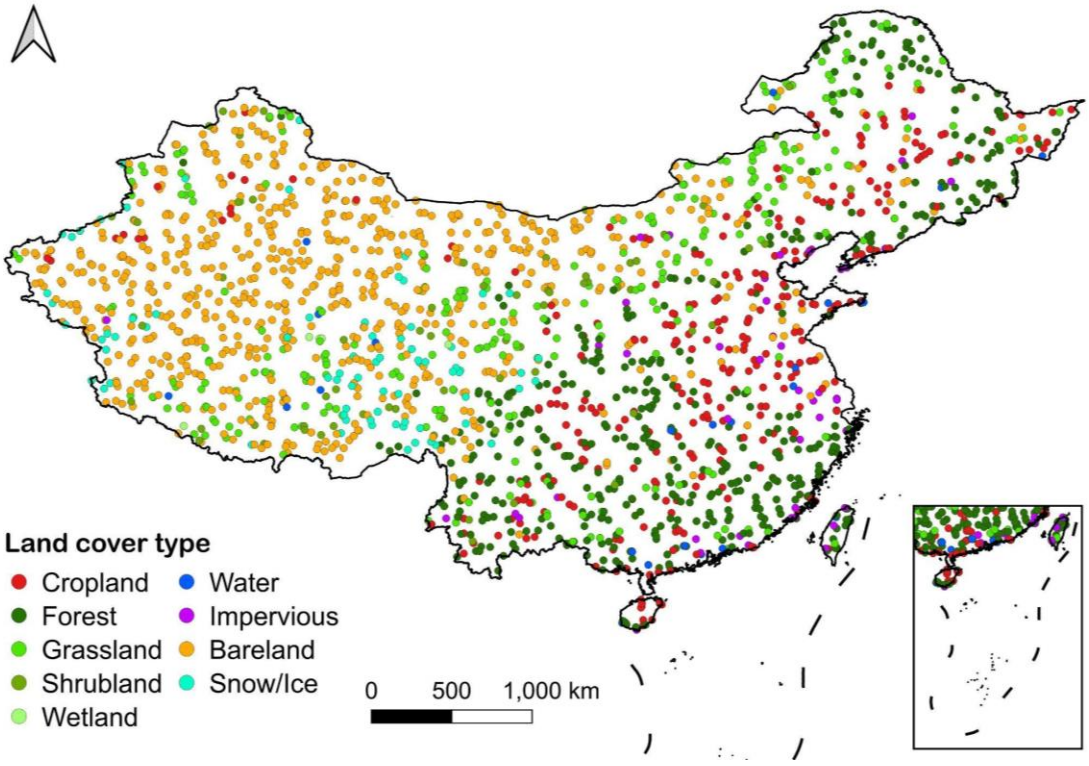

Figure S5. Distribution of global land cover validation sample set (GLCVSS) in China.

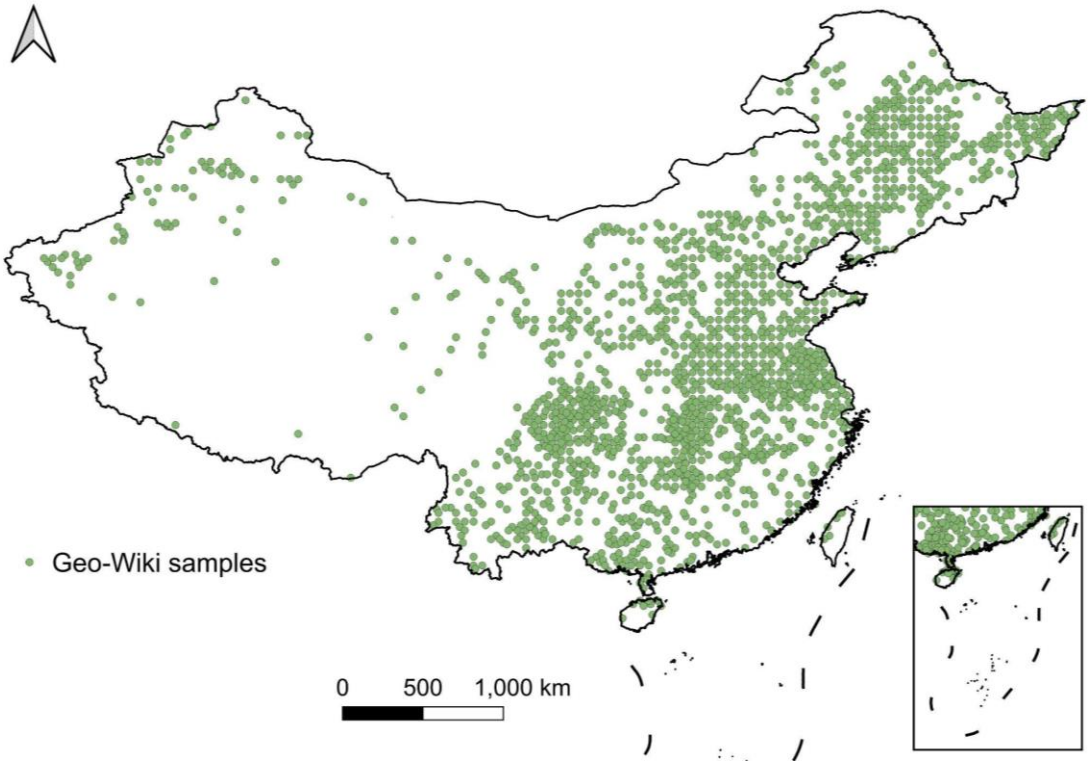

Figure S6. Distribution of GeoWiki cropland samples in China.

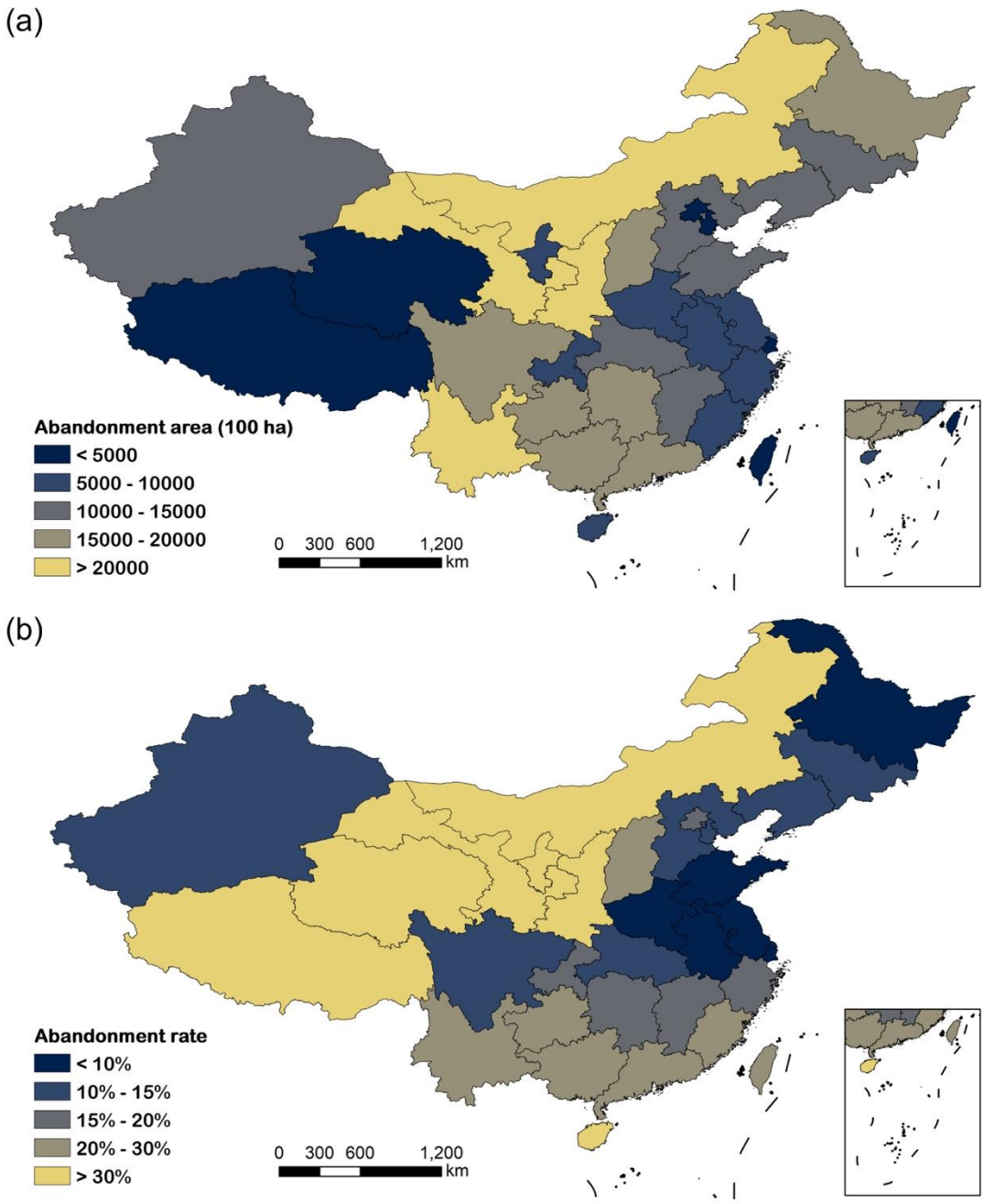

Figure S7. Provincial cropland abandonment in China between 1990-2015 of (a) area and (b) rate.

Table S1. A summary of the nine agricultural zones in China: their geographical and climatic conditions, growing seasons, cropping patterns, and major crops

Agricultural zones	**Geographical and climatic conditions**	**Growing seasons**	**Cropping patterns**	**Major crops**
Huang-Huai-Hai Plain	The largest alluvial plain of China being at the intersection of humid winds from the Pacific and dry winds from the interior of the Asian continent. Land is fertile and suitable for agricultural activity.	April to September	Double cropping	Wheat, maize, sorghum, millet, peanuts, sesame seed, cotton, apple, jujube
Loess Plateau	Has a continental monsoon climate. Winters are cold and dry, and most rainfall occurs during the summer. Annual precipitation is ~400 mm. Most areas are hills and plateaus covered by loess, with serious soil erosion.	May to September	Single cropping	Maize, millet, corn, sorghum, apple
Middle-lower Yangtze Plain	Centered on the extensive lowland plains of east-central China. Experiences a temperate climate with warm springs, hot summers, cool autumns, and relatively cold winters for the latitude.	April to October	Tripple cropping	Rice, maize, cotton, tea, rapeseed
Northeast China Plain	Under the humid continental climate zone with a hot rainy summer and cold dry winter. Suitable for mechanized farming, with thick and fertile soil and extensive amounts of arable land.	May to September	Single cropping	Maize, soybean, wheat, millet, sorghum, sugar beet
Northern arid and semiarid region	Has an arid desert climate. Has abundant light energy resources and good heat conditions, but precipitation is low, and sandstorms and alkalinization are severe	June to September	Single or double cropping	Wheat, melon, cotton, sugar beet
Qinghai Tibet Plateau	Belongs to the alpine plateau climate. Covered mainly by plateaus and mountains with 4000 meters above sea level. Difficult for cereal planting and only suitable for grazing.	May to September	Single cropping	Wheat, highland barley, potatoes
Sichuan Basin and surrounding regions	A lowland region in southwestern China. Experiences a subtropical monsoon climate with warm, hazy summers and chilly winter fog. Frost-free period is of 280-350 days.	April to October	Double or triple cropping	Rice, wheat, maize, red sage, rapeseed
Southern China	The only tropical economic crop planting area in the country. Experiences a subtropical and tropical climate with high temperatures and heavy rainfall particularly during the summer.	March to October	Triple cropping	Rice, rubber, various tropical fruits
Yunnan-Guizhou Plateau	A large mountainous region with rugged terrain. Climate gradually transitions from drier in the southwest to rainier in the northeast - in east-central Yunnan, parts of the Yungui Plateau experience a semi-arid climate, while most of Guizhou is classified as the humid subtropical region.	March to October	Double or triple cropping	Tobacco, tea, rubber, coffee

Table S2. Input features of multi-temporal metrics each year for the random forest classifier for estimating annual cropland probabilities.

Category	Feature	Description	Dimension	Source
Spectrum	10^{th}, 25^{th}, 50^{th}, 75^{th}, and 90^{th} percent quantiles of Blue, Green, Red, NIR, SWIR1, and SWIR2 bands of both growing and non-growing seasons	Spectral bands of Landsat data	6*5*2	Landsat
Spectral indices	10^{th}, 25^{th}, 50^{th}, 75^{th}, and 90^{th} percent quantiles of NDVI, NDSI, NDBI, NBR, and EVI indices of both growing and non-growing seasons	Normalized indices derived from spectral bands, which are calculated as: NDVI = (NIR-Red)/(NIR+Red) NDSI = (Green-SWIR1)/(Green+SWIR1) NDBI = (SWIR1-NIR)/(SWIR1+NIR) NBR = (NIR-SWIR1)/(NIR+SWIR2) EVI = 2.5*((NIR-Red)/(NIR+6*Red-7.5*Blue+1))	5*5*2	Landsat
Tasseled cap transformation indices	10^{th}, 25^{th}, 50^{th}, 75^{th}, and 90^{th} percent quantiles of brightness, greenness, and wetness indices of both growing and non-growing seasons	Tasseled cap transformation indices of spectral bands. Coefficients are derived from Crist (1985).	3*5*2	
Topography	Elevation	/	1	SRTM

Noted NIR and SWIR are short for the near-infrared and short-wave bands of Landsat data respectively. NDVI, NDSI, NDBI, NBR, and EVI are abbreviations for the normalized difference vegetation index, the normalized difference snow index, the normalized difference built-up index, the normalized burn ratio, and the enhanced vegetation index, respectively.

Table S3. Ten settings of LandTrendr parameters tested in this study.

Parameter	Settings									
	1	2	3	4	5	6	7	8	9	10
maxSegments	6	8	10	8	10	6	8	8	8	8
spikeThreshold	0.9	0.9	0.9	0.5	0.5	0.9	0.9	0.9	0.9	0.9
preventOneYearRecovery	TRUE	TRUE	TRUE	TRUE	TRUE	FALSE	TRUE	TRUE	TRUE	TRUE
recoveryThreshold	0.25	0.25	0.25	0.25	0.25	0.25	0.5	0.75	0.25	0.25
pvalThreshold	0.05	0.05	0.05	0.05	0.05	0.05	0.05	0.05	0.1	0.05
bestModelProportion	0.75	0.75	0.75	0.75	0.75	0.75	0.75	0.75	0.75	0.5

Noted other parameters are set as default as those provided in https://emapr.github.io/LT-GEE/lt-gee-requirements.html.

Table S4. Annual cropland classification results for each agricultural zone under different LandTrendr parameter settings.

Agricultural zone	Parameter settings with the highest F1 score	Statistics of F1 scores		
		Highest	Mean	Std
Huang-Huai-Hai Plain	3	0.89	0.87	0.01
Loess Plateau	4	0.83	0.80	0.04
Middle-lower Yangtze Plain	5	0.80	0.80	0.02
Northeast China Plain	4	0.88	0.87	0.01
Northern arid and semiarid region	6	0.71	0.62	0.06
Qinghai Tibet Plateau	8	0.67	0.59	0.10
Sichuan Basin and surrounding regions	5	0.78	0.76	0.02
Southern China	4	0.69	0.65	0.06
Yunnan-Guizhou Plateau	5	0.75	0.71	0.04

Std: standard deviations.

Table. S5. Pixel-wise accuracy of CACD calculated based on the annual validation samples. F1: F1 score. OA: overall accuracy. Kappa: Kappa coefficient. UA: user's accuracy. PA: producer's accuracy.

Year	F1	OA	UA	PA	Kappa
1986	0.76	0.91	0.77	0.75	0.70
1987	0.76	0.92	0.78	0.75	0.71
1988	0.77	0.92	0.78	0.75	0.71
1989	0.77	0.92	0.78	0.76	0.72
1990	0.76	0.92	0.78	0.75	0.71
1991	0.77	0.92	0.78	0.76	0.72
1992	0.78	0.92	0.78	0.77	0.73
1993	0.77	0.92	0.78	0.77	0.72
1994	0.78	0.92	0.78	0.77	0.73
1995	0.78	0.92	0.79	0.77	0.73
1996	0.78	0.92	0.79	0.77	0.73
1997	0.78	0.92	0.79	0.77	0.73
1998	0.78	0.92	0.79	0.78	0.74
1999	0.79	0.92	0.79	0.79	0.74
2000	0.79	0.93	0.79	0.80	0.75
2001	0.80	0.93	0.79	0.80	0.75
2002	0.79	0.92	0.79	0.80	0.75
2003	0.79	0.92	0.79	0.79	0.74
2004	0.79	0.93	0.79	0.80	0.75
2005	0.80	0.93	0.80	0.80	0.76
2006	0.80	0.93	0.80	0.81	0.76
2007	0.80	0.93	0.80	0.80	0.76
2008	0.80	0.93	0.80	0.81	0.76
2009	0.81	0.93	0.81	0.81	0.77
2010	0.81	0.93	0.80	0.82	0.77
2011	0.82	0.93	0.81	0.82	0.78
2012	0.82	0.94	0.81	0.83	0.78
2013	0.82	0.94	0.81	0.82	0.78
2014	0.82	0.94	0.82	0.82	0.78
2015	0.82	0.94	0.82	0.83	0.79
2016	0.81	0.93	0.80	0.82	0.77
2017	0.81	0.93	0.81	0.81	0.77
2018	0.81	0.93	0.81	0.81	0.77
2019	0.80	0.93	0.80	0.80	0.76
2020	0.80	0.93	0.80	0.80	0.76
2021	0.80	0.93	0.79	0.81	0.76
Mean	0.79±0.02	0.93±0.01	0.79±0.01	0.79±0.02	0.75±0.02

Table. S6. Accuracy of CACD for the year of change under different tolerance years.

Tolerance (years)	Accuracy
0	0.76
±1	0.79
±2	0.81
±3	0.84
±4	0.86
±5	0.87

References

Crist, E.P. (1985). A TM Tasseled Cap equivalent transformation for reflectance factor data. *Remote Sensing of Environment, 17*, 301-306